

# Phoenix: A Cryogenic High-Resolution 1-5 micron Infrared Spectrograph

Kenneth H. Hinkle, Randy Cuberly, Neil Gaughan, Julie Heynssens,  
Richard Joyce, Stephen Ridgway, Paul Schmitt, and Jorge E. Simmons

National Optical Astronomy Observatories†,  
P.O. Box 26732, Tucson, Arizona 85726-6732 USA

## ABSTRACT

We describe a cryogenic, high-resolution spectrograph (Phoenix) for the 1-5  $\mu\text{m}$  region. Phoenix is an echelle spectrograph of the near-Littrow over-under configuration without cross dispersion. The foreoptics include Lyot reimaging, discrete and circular variable order sorting filters, a selection of slits, and optics for post-slit and Lyot imaging. The entire instrument is cooled to 50 K using two closed cycle coolers. The detector is a Hughes-Santa Barbara 512x1024 InSb array. Resolution of 65,000 has been obtained. Throughput without slit losses (but including telescope losses) is 13% at 2.3  $\mu\text{m}$ . Recent results are discussed. Phoenix is a facility instrument of the National Optical Astronomy Observatories and will be available at CTIO, KPNO, and Gemini.

**Keywords:** infrared spectrograph, cryogenic spectrograph, echelle spectrograph, high resolution spectroscopy, infrared array detectors

## 1. INTRODUCTION

High resolution spectroscopy in the infrared has been a major scientific interest at NOAO since the construction of the Kitt Peak National Observatory (KPNO) 4 m telescope in the early 1970's. At that time the forefront instrument for astronomical, high resolution, infrared spectroscopy was the Fourier transform spectrometer (FTS). The FTS that was installed at the 4 m telescope<sup>1</sup> was highly productive setting the foundation for much of the research now being carried out using infrared spectroscopy<sup>2</sup>. While Fourier spectroscopy has many merits, it is based on rapidly sampling single element infrared detectors. With the advent of infrared arrays it was recognized that a cryogenic spectrograph employing a grating as the dispersive element and an infrared array as the detector can be orders of magnitude more sensitive than a FTS<sup>3</sup>.

This report describes the design, construction, and performance of an infrared optimized, cryogenic, echelle spectrograph we have named Phoenix. The scientific requirements of the KPNO user community demanded a high-resolution IR spectrometer with minimum resolving power ( $R=\lambda/\Delta\lambda$ ) of 100,000 over the 1-5  $\mu\text{m}$  wavelength range. The size and weight of the instrument were constrained by the requirement that it had to be carried on the 2.1 and 4 m telescopes. As a result the weight had to be less than a ton and the vacuum enclosure could not extend more than 1 m below the telescope focal plane. The observatory was also coming under increasing budget pressure which dictated building as simple an instrument as possible that was capable of achieving the scientific goals.

## 2. DESIGN PARAMETERS

Bingham<sup>4</sup> provides the relation between slit width in arcseconds (S) and resolution (R) for astronomical grating spectrographs. By using the grating equation converted to the case of an echelle used at Littrow this equation can be expressed as

$$S = (412530W \sin\theta)/(DR) \quad (1)$$

where W is the illuminated width of the grating in the plane of the grating, D is the diameter of the telescope, and  $\theta$  is the grating angle. The largest commercial available gratings are R2 echelle rulings (blaze angle 63.<sup>o</sup>4 ) in

---

Other author information: Send correspondence to K.H.H. K.H.H.: E-mail: khinkle@noao.edu; R.C.: E-mail: randyc@noao.edu; N.G.: E-mail: gaughan@noao.edu; J.H.: E-mail: julieh@noao.edu; R.J.: E-mail: rjoyce@noao.edu; S.R.: E-mail: sridgway@noao.edu; P.S.: E-mail: pschmitt@noao.edu; J.E.S.: E-mail: simmons@noao.edu

†Operated by the Association of Universities for Research in Astronomy, Inc. under cooperative agreement with the National Science Foundation.

lengths up to 408 mm. For the 2.1 m telescope, this gives a slit-width resolution product,  $SR$ , of 71665 ; for the 4 m  $SR = 39600$ . At  $R=10^5$  the slit width is a good match to the seeing at the 2.1 m. At the 4 m, the  $R=10^5$  slit width is a good match to adaptive optics. Lower resolution is of course possible by using wider slits.

Phoenix consists of two basic units, a foreoptics module and a spectrograph module. Each module could be optically designed, assembled, and tested independently and later coupled by means of a distance adjustment, axial tilt, and decenter of axes. The foreoptics reimages the telescope secondary at a Lyot stop and the field onto the slit. The spectrograph unit consists of a R-C camera-collimator which illuminates an echelle grating and then reimages the spectrum on the array. We employed a design with the collimator and camera combined into a single Ritchey-Chretien (R-C) telescope because in a system of this type the detector pixel scale has a one-to-one relation with the slit width. The foreoptics, which reimage the secondary at a Lyot stop, can be designed to match an arbitrary input focal ratio from the telescope, but the output focal ratio must be the focal ratio of the R-C collimator. A collimator focal ratio of 7.5 gives a 2 pixel slit width for the array used in Phoenix, matching the desired  $SR$  product. A R-C collimator of  $f/7.5$  is also readily fabricated and relatively compact.

The remainder of the design was driven by the need to produce a relatively compact instrument with as little development work as possible. A standard echelle grating was selected instead of investigating developing grating technologies. Cross dispersion was not included for multiple reasons. First, at  $R=10^5$ , arrays as large as 1024 pixels in the dispersion direction do not allow coverage of the free spectral range for obtainable groove spacings. Second, the thermal background increases rapidly from  $\sim 2 \mu\text{m}$  to  $5 \mu\text{m}$ . The exposure time in the 3-5  $\mu\text{m}$  thermal infrared can not be optimized for multiple orders. Third, a classical cross dispersed design was both too large and too complex for the cost/size/weight boundaries of this instrument. Finally, refractive cross dispersion over a wavelength range as large as 1-5  $\mu\text{m}$  would require a large number of prisms and presented a design challenge that exceeded the scope of the project. In the infrared it is required to have a spatially extended slit for sky subtraction. The longest slit possible was desirable for mapping of extended features, for instance  $\text{H}_2$  emission from nebulae. A slit length of 1 arcminute on the 2.1 m was the design goal.

The design process resulted in the instrument shown conceptually in Figure 1. The entire instrument illustrated is operated at cryogenic temperatures. In addition to the basic units, three imaging systems are included for acquisition, guiding, and diagnostics. One when placed behind the slit images the field, the second images the Lyot stop. A third in the foreoptics contains a dichroic that passes the visible light out the side of the dewar to a CCD guide camera. All the mechanisms are under computer control and operated at the user level by a graphical user interface window.

### 3. OPTICAL DESIGN

The optical modeling was done for the nominal 'f/15' focus of three telescopes: the Kitt Peak 2.1 and 4 m and the Gemini 8 m. The central obstruction of the 2.1 and 4 m telescope is about a 0.3 diametrical ratio and this was taken as a design norm. All telescopes were assumed to be focused at the same plane in the instrument. The optics govern the pupil and the image planes. Masking at a reimaged secondary (Lyot stop) is provided. The optical modeling was done using the ACCOS package<sup>5</sup>.

#### 3.1. Foreoptics

The conceptual design is contingent on the foreoptics converting the input telescope focal ratio number to that of the collimator;  $f/15$  to  $f/7.5$  in this case. Using two sets of triplets it is possible to achieve  $f$ /number conversion from 1 to 5  $\mu\text{m}$ , to form a well separated Lyot stop area, and to maintain field<sup>6</sup>. Each triplet consists of two lenses of the same material and one lens with a slightly different index of refraction. For the 1-5  $\mu\text{m}$  region,  $\text{BaF}_2$  and  $\text{CaF}_2$  were selected with a close  $\text{CaF}_2$  and  $\text{BaF}_2$  doublet and a much more distant  $\text{BaF}_2$  singlet.

The diameters of the foreoptics lenses, typically 25 mm, are oversized to prevent vignetting or ghost reflections from the mounting hardware. The thicknesses are mainly dictated by curve and diameter and the requirement that there be sufficient edge and center thickness. The triplet design is quite forgiving regarding tolerances. This not only aids design and assembly but increases performance stability since the optics are assembled at room temperature and used at cryogenic temperature.

The foreoptics are focused on the entrance slit of the spectrograph. The focus changes with wavelength by several mm over the 1-5  $\mu\text{m}$  range. In addition, the focus of the foreoptics is changed by the addition of filters near the Lyot space or by using a circular variable filter (CVF) near the slit. These changes are corrected by refocusing the telescope.

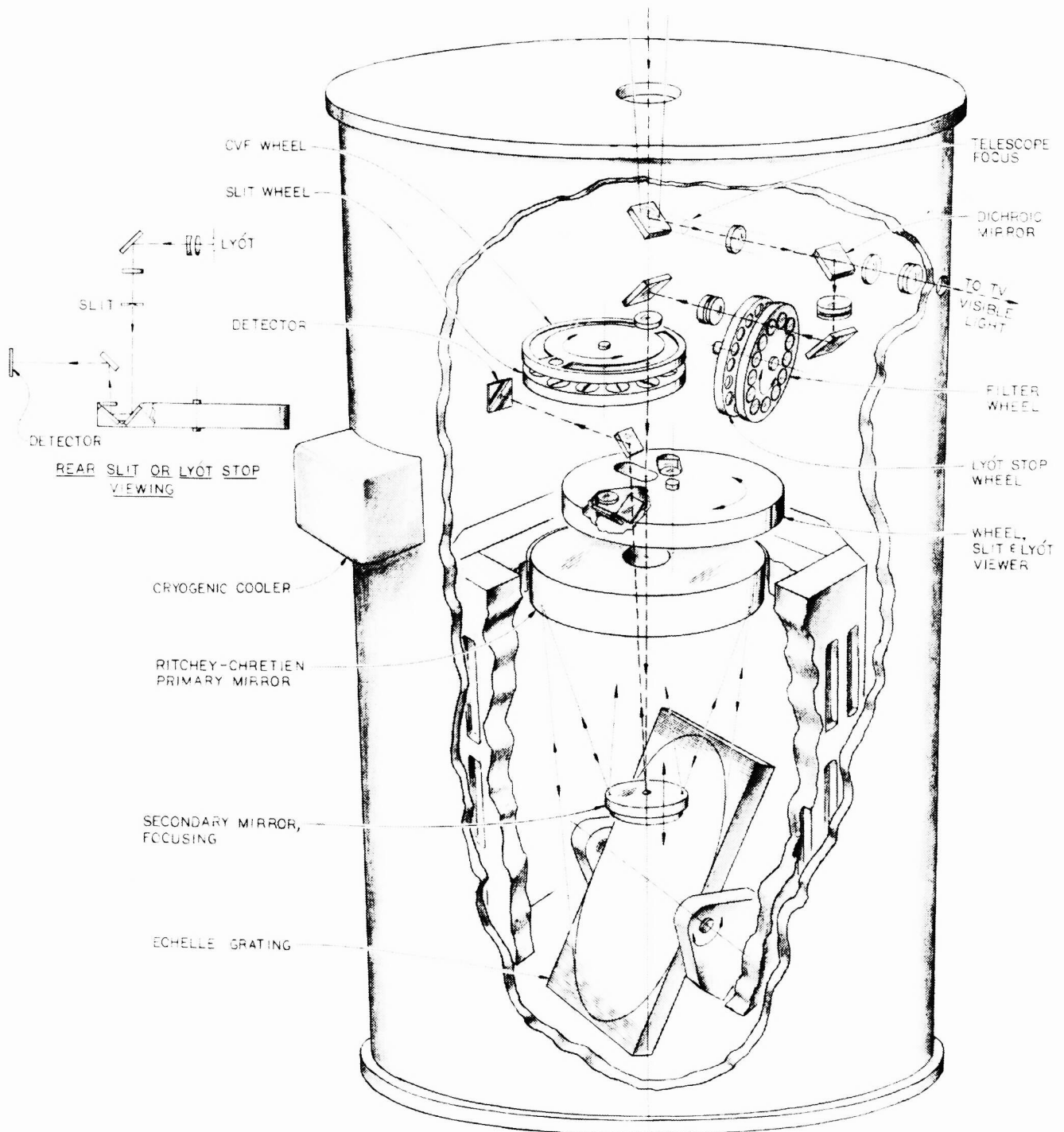


**Figure 1.** A schematic drawing of the Phoenix layout. The detail to the left shows the conceptual layout of the post-slit and Lyot viewer optics. An open hole in this wheel, as shown in the main part of the illustration, allows light into the collimator.

The foreoptics design is given in Table 1. The foreoptics also contain a plano-concave ZnSe lens mounted immediately behind the slit. This lens images the pupil on the grating. Since ZnSe has a high index of refraction this lens is anti-reflection (AR) coated. The CaF<sub>2</sub> and BaF<sub>2</sub> lenses are not coated since a suitable broad band coating that significantly enhances the throughput over the entire 1-5  $\mu\text{m}$  range was not available for this low refractive index material.

**Table 1.** Foreoptics. All dimensions are in mm.

Element	Distance	Material	Note
Window	8.0	CaF <sub>2</sub>	diameter 76
Window-Tel focal plane	154.8	vacuum	
Tel focal plane-L1	43.7	vacuum	
L1	3.0	BaF <sub>2</sub>	R1 CX 159.66 $\pm$ 1.0 R2 CX 305.4 $\pm$ 2.0
L1-L2	116.34	vacuum	
L2	3.0	CaF <sub>2</sub>	R1 CC 1842 $\pm$ 35.0 R2 CC 55.93 $\pm$ 0.15
L2-L3	3.95	vacuum	
L3	4.25	BaF <sub>2</sub>	R1 CX 490.8 $\pm$ 2.5 R2 CX 39.87 $\pm$ 0.11
L3-Lyot stop	74.75	vacuum	see note
Lyot stop-L4	30.25	vacuum	see note
L4	4.45	BaF <sub>2</sub>	R1 CX 46.76 $\pm$ 0.14 R2 CX 43.05 $\pm$ 0.12
L4-L5	2.94	vacuum	
L5	3.0	CaF <sub>2</sub>	R1 CC 35.2 $\pm$ 0.10 R2 CC 774.0 $\pm$ 8.0
L5-L6	68.35	vacuum	
L6	3.25	BaF <sub>2</sub>	R1 CX 24.22 $\pm$ 0.1 R2 CC 187.86 $\pm$ 1.0
L6-CVF	10.0	vacuum	
CVF	3.175	silicon	
CVF-Slit	4.98	vacuum	
L7	1.8	ZnSe	R1 Plano R2 CC 178.69 $\pm$ 2.0

Note: The distance L3 to Lyot stop, Lyot stop to L4 given here is for the 2.1 m telescope at a wavelength of 2.5  $\mu\text{m}$ . The Lyot stop diameter and position change slightly with telescope and wavelength but the L3-L4 distance is fixed.

The exit pupils located at the secondary mirrors on the three telescopes for which Phoenix was planned are imaged in different planes. Fortunately, the separation of the planes is not much, covering a total span of only 5 mm. The typical diffractive depth of focus,  $\pm 1$  mm, allows five stops to cover the 1-5  $\mu\text{m}$  range.

Phoenix was designed for order sorting using either custom filters in the Lyot space or a CVF near the slit. Custom filters can be purchased with high throughput (50-80% depending on the central wavelength), nearly rectangular band shape, and exceedingly good out-of-band blocking. As a result custom order sorting filters are preferred over the CVF. In addition, by wedging the custom filters, spectral fringing can be largely suppressed. The custom filters have FWHM bandpasses of 100  $\text{cm}^{-1}$  and are blocked to  $10^{-4}$  or more for wavelengths more than  $\pm 88$   $\text{cm}^{-1}$  from the band center to prevent spectral leakage from adjoining orders.

### 3.2. Collimator-Grating

The collimator-grating module is composed of a hyperbolic primary and a hyperbolic secondary. The collimator is also the camera, with the optical axis of the foreoptics assembly steering light into the collimator-grating secondary at 2.6 mm over its optical center and at an angle of 1.9° CCW with respect to its optical axis. In this way, the foreoptics initial axial ray becomes the chief ray of a collimator-grating monochromator operating with field. A limitation of this design is that the 2.675 mm over axis at the center of the secondary is 11.02 mm off axis at the

distance of the slit and detector from the secondary. Thus the greatest possible size of the input field is  $\pm 11$  mm. Since this must be a mechanical assembly the size is actually considerably less than this. The slit length in Phoenix is 4.4 mm. The field size could be increased by increasing the off axis angle. However, increasing this angle rapidly increases the aberrations.

Since the path through the collimator is double, the tolerances are halved. The double path over-and-under the axis cancels coma but duplicates astigmatism. Notwithstanding, the ray tracing software found diffraction limited spectral images with acceptable (pixel limited) spatial imagery. As with any R-C telescope, the alignment and tilt of the secondary to the optical axis of the primary is critical. Decentering and tilt due to flexure were modeled to determine the instrumental stiffness to hold the components within the limits shown by tolerance runs.

The diffraction depth of focus of the collimator grating assembly used in double pass is  $\pm 0.125$  mm at the entrance or exit image planes. Due to the magnification of the optics, this corresponds to a motion of the secondary of  $\pm 10$   $\mu\text{m}$ . Silicon was selected for the collimator optics because of the dimensional stability and large thermal conductivity<sup>7</sup>. Since the collimator frame is aluminum, the focus of the collimator changes from room temperature to the cryogenic operating temperature and the secondary was designed to be focusable. The optical layout of the collimator is given in Table 2.

Over-under echelle geometry is well understood<sup>8</sup>. One result is that the direction of dispersion and the image position of the slit are not perpendicular. In Phoenix the array has been rotated to make the slit spectral image lie along rows. To account for field curvature, the detector has also been tilted by  $7.8^\circ$  CCW from the normal to the outgoing beam.

**Table 2.** Collimator Optics. Units in mm.

primary paraxial radius of curvature	689.16 $\pm$ 3
	hyperbolic eccentricity 1.023
secondary paraxial radius of curvature	269.163 $\pm$ 1.2
	hyperbolic eccentricity = 1.729
primary to secondary	241.909
secondary to slit/detector	433.0

The free spectral range of an echelle grating is given by the groove spacing with larger spacings giving less free spectral range<sup>9</sup>. The coarsest available grating, 31 lines  $\text{mm}^{-1}$ , has a free spectral range of  $176$   $\text{cm}^{-1}$ , or 1.7 percent at  $1$   $\mu\text{m}$ . Filters of this width are commercially obtainable. Coverage of the free spectral range requires a maximum tip at the longest wavelengths of  $\pm 6^\circ$ . Cost considerations dictated the selection of a replica grating. A replica on an aluminum substrate is currently being obtained. The original silicon substrate<sup>7</sup> had a coefficient of expansion that was incompatible with the replication epoxy.

### 3.3. Collimator Baffling

The design of the baffling is critical to the collimator design. The baffling must keep light from the grating from falling directly on the detector. The center of the secondary acts as a mirror reflecting whatever is in front of it and will not only reflect the surface of the primary but also light entering the central hole through the entrance slit. The detector also reflects some light back into the collimator. Direct light from the grating is stopped with baffles on the face of primary and around the secondary. The direct images of the entrance slit and the detector's surface are eliminated with a central stop on the face of the secondary. Overall, approximately 30 percent of the input light is obscured by the baffling.

The baffle cone that fits over the secondary has a minor inside diameter of 70 mm, the same as the outer diameter of the secondary, and a major inside diameter of 84 mm. The height of this truncated cone is 29 mm. The walls of the baffles are threaded and black anodized to reduce unwanted reflections. The baffle cone fitted into the central hole of the primary has a major outer diameter of 78 mm and a minor outer diameter of 54 mm. The minor inner diameter is 52 mm. The length of the truncated cone is 102.5 mm. The hole at the center of the primary is 45 mm in diameter. This baffle is also threaded and black anodized. The center of the secondary contains a button-type



**Figure 2.** The primary (facing viewer) and secondary mirrors in the collimator. The grating fits tightly against the secondary and has been removed for this photograph. The central baffle of the secondary can be seen in reflection in the primary as can the secondary baffle cone. The primary baffle cone is seen in the middle of the primary. Light absorbing aluminum foam can be seen mounted on the collimator box. The secondary support structure with the push-pull alignment screws as well as the bottom of the secondary focus mechanism are also shown. The secondary focus lead screw is housed in the enclosure at the extreme right.

stop of 13 mm diameter. This button is a black anodized plate tipped to the side to reflect any non-absorbed light to the side of the collimator. Figure 2 shows the interior of the collimator.

### 3.4. Guider and Slit/Lyot Viewer Optics

For the purposes of fitting the optical package into the dewar a number of flat mirrors had to be used to fold the optical path. The second of these in the foreoptics was replaced with a dichroic mirror that is 96% or more reflective from 1.2 to 5  $\mu\text{m}$ . The dichroic transmits over 50% of the light from 480 to 650 nm in the visual. Light transmitted by the dichroic passes through three reimaging lenses and an exit window in the dewar. An intensified CCD mounted to a standard 150 mm TV lens placed about 20 cm from the window refocuses the visual light for on-axis guiding. At the 2.1 m telescope it is possible to guide on early-type stars as faint as 14th magnitude.

Two sets of diagnostic optics can be moved in behind the slit. One is a lens for imaging the Lyot stop on the infrared detector. This must be used with a matching lens in the slit wheel. Imaging of the Lyot space allows an image of the telescope secondary to be aligned in the Lyot stop. The other diagnostic package is a triplet of lenses which images the slit plane onto the infrared array. This is used for acquisition of infrared objects that are visually faint as well as for a number of set up and diagnostic tasks such as focusing the telescope. The triplet is achromatic from 0.6 to 3  $\mu\text{m}$ . The optical parameters for these systems are given in Table 3. These lens systems change the scale of the image compared to that obtained with the spectrograph. For the slit viewer the scale is 1.6 times larger than in spectroscopy mode ( imaging scale = 0.24 arcseconds per pixel on the 2.1 m; spectroscopy scale = 0.35 arcseconds per pixel on the 2.1 m).

## 4. MECHANICAL DESIGN AND FABRICATION

The mechanical components consist of several units: the vacuum enclosure, instrument support and radiation shielding, the instrument structure, and the mechanisms. Most of the instrument is constructed from T6061-T651 aluminum that has been uphill quenched to relieve stresses<sup>10</sup>.

Twenty-five mm thick aluminum plate was rolled and welded into a cylinder of 74 cm inside diameter by 92.1 cm high. This tube was heat treated and slots cut into the cylinder for bosses. End flanges and bosses were welded in place. The flanges were machined to the correct diameter and the dewar was anodized. The inside of the dewar was then milled, the faces of the flanges machined, the O-ring grooves added, and the bosses finished. End plates were manufactured out of 3.8 cm thick aluminum plate. The inside of the dewar was polished to lower the emissivity. The exterior of the finished dewar was painted for cosmetics.

The cryogenic instrument package is supported by a 9.5 mm thick by 55.3 cm long G-10 fiberglass ring of 66 cm diameter that is mounted at one end to the dewar and at the other end to an aluminum ring. This ring holds the instrument structure near its center of gravity. The radiation shielding is aluminum sheets of 1.6 mm thickness. An inner radiation shield covers the instrument and is actively cooled to cryogenic temperatures. A number of holes exist in this shield for mechanical feed-throughs, light paths, and the refrigeration feed-throughs. These holes have ample clearance with no attempt at radiation baffling. Between this shield and the dewar wall there is a thermally floating outer radiation shield. With the instrument at an operating temperature of 50 K, the outer shield reaches radiative equilibrium at 220 K.

The support for the cryogenic instrument package itself is a ring that hangs from the fiberglass ring. This ring bolts to the collimator frame, actually a closed rectangular box. The foreoptics are supported on a two level plate which stands on a ring bolted to the main support ring. The instrument package with the radiation shields removed

**Table 3.** Guide/Acquisition/Diagnostic Optics

Unit	Element	Distance	Material	Note
Visible Guide Channel	Tel F.P.-BaF <sub>2</sub>	43.7	vacuum	IR+VIS light
	IR L1	3.0	BaF <sub>2</sub>	R1 CX 159.66 R2 CX 305.4
	BaF <sub>2</sub> -dichroic	90.0	vacuum	
	dichroic	5.0	silica?	IR reflected
	dichroic-L1	25.0	vacuum	VIS light only now
	L1	4.25	BK7	R1 71.45 CX R2 127.0 CX
	L1-L2	47.72	vacuum	
	L2	3.0	F2	R1 83.0 CC R2 184.6 CC
	L2-L3	1.0	vacuum	
	L3	3.0	F2	R1 75.27 CC R2 55.55 CX
Lyot Viewer	L3-window window	140.2 4.765	vacuum silica	
	Slit-L1	0.8	vacuum	
	L1	3.0	CaF <sub>2</sub>	186.9 equiconvex
	L1-L2	157.3	vacuum	
	L2	4.0	CaF <sub>2</sub>	39.67 equiconvex
Slit Viewer	L2-detector	102.0	vacuum	
	slit-L1	99.5	vacuum	
	L1	4.0	BaF <sub>2</sub>	R1 40.342 CX R2 33.82 CX
	L1-L2	1.1	vacuum	
	L2	2.0	CaF <sub>2</sub>	R1 42.8 CC R2 23.69 CC
	L2-L3	1.23	vacuum	
L3	4.0	BaF <sub>2</sub>	R1 48.99 CX R2 52.41 CX	
L3-detector	154.9	vacuum		

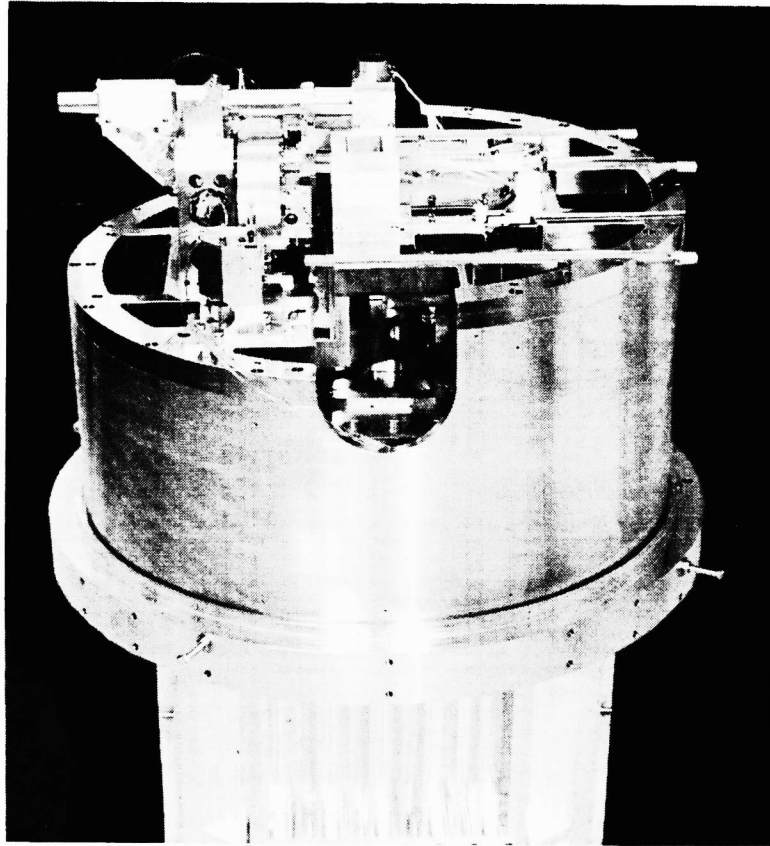


**Figure 3.** The instrument (95 cm tall by 64 cm diameter with weight 200 kg) is shown with the dewar and radiation shields removed. The collimator is housed in the rectangular section at the bottom. The instrument is supported by the ring at the middle. The cylinder above this is the support of the foreoptics bench. Some of the foreoptics structures can be seen on the two level bench. The U shaped opening is for a closed-cycle-cooler cold head. Everything shown is operated at 50 K.

is seen in Figure 3.

As mentioned above, no special care has been taken to make the radiation shields light tight since the instrument itself is designed to be light tight. The instrument design is basically a series of connected tubes. Light tight seals, employing lead O-rings, are used where one unit is attached to the next or where two surfaces meet. Inside surfaces which are potentially exposed to the light path are made to be non-reflective. This is done by threading or, on the large collimator sections, by covering with expanded aluminum foam. In addition these surfaces are hard black anodized<sup>11</sup> (Figure 2).

#### 4.1. Foreoptics Mechanisms

The foreoptics contains two modules each holding two wheels mounted back-to-back. One holds the filter and Lyot wheels and the other the CVF and slit wheels. All four of these mechanisms contain a diode and detector mounted on opposite sides of a flange for finding the zero point of the mechanism. A fifth mechanism holds the post-slit viewing optics. All the mechanisms in Phoenix are operated with external motors and encoders and are connected to the motors by hollow fiberglass rods. Ferro-fluidic feed-throughs are used to exit the dewar.

The wheel for custom echelle order sorting filters is the first mechanism in the light path, situated immediately in front of the Lyot stop. The wheel has 13 positions, 12 for filters and one left open. The Lyot wheel holds 16 stops used to mask the edges of the reimaged telescope optics. In addition to the normal Lyot stops the wheel also contains one dark slide and some Hartmann-type masks for alignment and intensity reduction in imaging mode. Both the filter and Lyot wheels are latched with a pawl for precise positioning.

A wheel with a circular variable filter (CVF) is located immediately in front of the slit. The CVF must be close to the slit. The angular range that light can pass through on the wheel must be limited. Since the CVF is continuously variable, the CVF wheel can be turned to any position. The entrance slit for the spectrograph is not a continuously variable jaw but is a series of slits in a wheel. All the slits have the same length, 4.4 mm. Three widths are provided, 54  $\mu\text{m}$  (2 pixels), 81  $\mu\text{m}$  (3 pixel), and 107  $\mu\text{m}$  (4 pixel). A pupil reimaging lens is mounted behind each slit. The slit wheel also has an open position which is used for imaging, a dark slide, and several diagnostic positions (e.g. a pin hole and a Lyot viewing lens). The slit wheel uses a pawl which positions the slits with repeatability of 5  $\mu\text{m}$  or better.

Immediately behind the slit, filling the space between the foreoptics and the collimator, and beside the detector is the post-slit viewer wheel. This is a thick wheel that has four positions. One is a dark slide that closes in front of the detector. Another is a hole that allows light to enter and exit the collimator. The other two positions are for the slit viewer and Lyot viewer described above. These are illustrated in Figure 1.

## 4.2. Spectrograph Collimator-Grating

There are two moving parts in the collimator-grating assembly of the spectrograph module, a collimator focus mechanism and the grating rotation. The focus mechanism, parts of which can be seen in Figure 2, is driven by a lead-screw which in turn pushes a spring loaded lever resting on the bottom of a shaft attached to the secondary. The design allows for controlled motion of the secondary over a range of 3 mm with a precision of a few  $\mu\text{m}$ . The collimator is focused by measuring spectra of an emission line from a hollow cathode source mounted outside the dewar. With the appropriate blocking filter and grating angle, spectra are observed with the collimator secondary at several focus positions. Once the focus settings bracketing a good focus are found, observations are taken stepping up to the correct focus position in small steps. The sequence is halted when the hollow cathode line becomes symmetric and reasonably narrow. The best focus in 1997 was 3.2 pixels. We find that it is necessary to refocus the collimator after cycling between room and cryogenic temperatures and after significant handling of the instrument.

The grating angle can range between 57 to 69°. The grating is supported by a pedestal cut into the back side of the substrate<sup>12</sup>. This pedestal is held in a circular clamp on an aluminum base plate. The sides of the plate hold axes which are in turn supported by tapered roller bearings. The grating is positioned by a worm gear on the axis. The grating must be positioned to a few arcminutes. However, once positioned, it must remain in place to a small fraction of an arcsecond. To hold the grating in place, the mechanism has been counter weighted using tungsten weights. Tungsten was selected because it is both dense and relatively inexpensive, but since it is difficult to work, slices of commercially supplied rod are held in aluminum tubes. In addition, a small solenoid operated brake pushes against the grating carriage and releases when the solenoid is activated during a grating motion.

## 4.3. Refrigeration

Phoenix is cooled with two Leybold 65 W closed cycle coolers run off a single compressor. No liquid cryogenics are used. The first stages of the cold heads are mounted with multiple thick copper braid to copper blocks attached to the collimator assembly. The instrument requires three days to cool from room temperature to operating temperature. Warming to room temperature takes 24 hours using resistive heaters mounted onto the copper blocks. Typically, after warming with the heaters, the instrument is backfilled with warm dry nitrogen several hours before opening to prevent any possibility that frost might form on more thermally isolated components. The cold heads are mounted across the dewar from each other with only flexible connections into the dewar. Vibration damping material is used under the cold head mounting bolts and bellows extend the dewar vacuum enclosure to the cold head. Unlike previous NOAO instruments<sup>13</sup> the heads are not synchronized. No detectable vibration from the cold heads can be measured at the telescope.

In addition to the main instrument cooling, the second stage of the cold heads is connected with a thin copper braid to the detector mount. Temperature sensing diodes and resistive heaters on the detector mount are used by a feed back system to maintain the detector temperature at  $28 \pm 0.1$  K. The rest of the instrument has an equilibrium temperature of 50 K. Cooling below 65 K is required since the InSb array is sensitive to radiation with wavelength as long as 5.6  $\mu\text{m}$ .

## 5. INTERFACE/MOUNTING UNIT

A spacer and calibration unit goes between Phoenix and the telescope. The interface unit for the NOAO 2.1 and 4 m telescopes is a 54.6 cm diameter cylinder 35 cm high including end plates for mounting to the telescope and to the Phoenix dewar. The NOAO interface unit has three manually controlled movable parts. A slide closes off the unit to protect the dewar window. The interface unit houses an integrating sphere with refocusing optics that produce a  $f/15$  beam, which may be directed into Phoenix by moving a mirror into the beam. The integrating sphere is illuminated by a tungsten filament bulb to generate flat field calibration frames. A port exists to the outside of the unit to allow other sources to be used as well. Last is a slide mechanism with one out-of-beam and two in-beam positions. One position places a gas cell over the window. The gas cell is 15 cm long filled with 30 Torr CO producing 10% deep absorptions in the  $2.3 \mu\text{m}$  first-overtone lines. The position of the gas cell is such that either star light or light from the integrating sphere can be used with the cell. The other position of the slide places a Th-Ne-Ar hollow cathode source over the window to provide sharp spectral lines for focusing the collimator.

## 6. DETECTOR ARRAY, ELECTRONICS, AND SOFTWARE

The detector array, from the Aladdin project<sup>14</sup>, is a  $1024 \times 1024$  InSb array with  $27 \mu\text{m}$  pixels. The Aladdin arrays are divided into four  $512 \times 512$  quadrants. The output from the Phoenix collimator is a 4.7 by 28 mm (174 by 1024 pixel) band. As a result only two quadrants are activated on the array in use. To keep the resultant image files as small as possible the operating microcode reads out only a  $256 \times 1024$  subarray containing the illuminated region. The Phoenix array has a dark current of  $0.15 \text{ electron pixel}^{-1} \text{ s}^{-1}$  and a read noise of 60 electrons. The gain is  $8.3 \text{ electrons ADU}^{-1}$ . Multiple readouts can be used to achieve a read noise of  $\sim 35$  electrons.

The array is controlled by the NOAO Wildfire instrument control system<sup>10,15</sup>. The control system generates the array clock waveforms and transfers the digitized pixel data from the instrument to a digital signal processor (DSP) located in an off instrument electronics rack. The instrument controller, sequencer, and instrument fiber transmitter are integrated into the electronics box on the instrument. Two way communications between the electronics box and the DSP is via optical fibers. The DSP uses transputers for assembly and hardware coadding of images before transmitting through an S-Bus to VME interface to a SUN host computer, which is also the user interface. User commands, such as mechanism control or initiating observations, are sent from the SUN through the DSP to the instrument controller transputer. The instrument electronics box also contains motor control, temperature control, housekeeping, precision reference/clock drivers, preamplifiers, and the signal processor/analog to digital converters.

The Wildfire user interface on the SUN is implemented within the TCL (tool command language) environment. The Phoenix application contains dedicated scripts for those functions specific to the instrument during normal operation, as well as for diagnostic purposes, such as logging the temperature sensor readings during the cool-down and warm-up cycles. The data appear in the NOAO Image Reduction and Analysis Facility (IRAF) environment for analysis by the user and archiving to tape within IRAF. This permits data analysis to proceed in parallel with instrument operation within different windows on the same workstation. A GUI constructed over the Wildfire interface provides a graphical display of the light path within the instrument, control of and status read back of the individual mechanisms, and a status board of the relevant observing parameters selected by the user. Diagnostic information, such as a time plot of selected temperature sensors, is also available through the GUI.

Although Wildfire was designed to provide high speed read out of IR arrays, this capability is not required for high resolution spectroscopy. The well depth of the Aladdin array is 100,000 electrons. The fastest readout possible with the Phoenix electronics is 1 second. With spectral dispersion of 200000 per pixel and a spatial dispersion of  $\sim 5$  pixels this readout time allows spectra of sources as bright as magnitude -4 in the  $1.6 \mu\text{m}$  region (peak throughput) to be observed on the 2.1 m telescope.

## 7. INSTRUMENT PERFORMANCE

First light was in June 1996. Phoenix has been used extensively since that time on both the KPNO 2.1 m and 4 m telescopes. At the time of this report two areas of the instrument were still being optimized, the motor-encoder control of the mechanisms and the collimator-grating unit. Both will be reported on in detail elsewhere. The instrument performance reported here will be enhanced by up-upgrades in these areas.

The slitless throughput in the  $1.6 - 2.5 \mu\text{m}$  region is 13%, in good agreement with calculations of the efficiency of the optical elements. Slit losses are typically near a factor of 3, somewhat higher than anticipated. As of March 1997,

the scattered light in opaque narrow lines of point sources is 2.5%; on broad lines the scattered light is slightly less, about 2%. At least part of this was contributed by peeled areas on the the silicon substrate grating and is expected to decrease when the aluminum substrate grating is used. With a 2-pixel slit, the best monochromatic images have a FWHM of about 3 pixels, corresponding to a spectral resolution of 65000. Resolution should be increased with the aluminum substrate grating. The mechanical stability of the instrument, which is crucial to high-resolution spectroscopy, is excellent. Flexure of the spectrograph is of order 1 pixel within a zenith distance of 60°. All-sky radial velocity accuracy of 1 km s<sup>-1</sup> has been obtained over the course of a night. In addition, there is no measurable flexure between the spectrograph slit and the external guiding CCD camera, ensuring a stable fiducial for acquisition and telescope guiding.

Light leakage in the instrument is very small. There is no detectable light leak in the foreoptics of the instrument. When taking long spectral exposures, the brightest sections of the array see a background rate of 0.7 electron pixel<sup>-1</sup> s<sup>-1</sup>. The median background over the entire detector is 170 ADU pixel<sup>-1</sup> in 1 hour, corresponding to 0.4 electron pixel<sup>-1</sup> s<sup>-1</sup>. We have not yet resolved this into array dark current versus light in the instrument, but any possible light leaks are in any case not limiting the performance. Furthermore, there are no ghosts or glints of starlight in the foreoptics. There is a low level ghost reflection in the collimator, but this has not been a problem in reducing the data. A reflection on a shiny surface near the detector is suspected.

Data are taken using conventional longslit IR spectroscopic techniques<sup>16</sup>. Point sources are observed at two or more positions along the slit; adjacent observations are differenced to cancel out features such as dark current or sky emission common to the two exposures. These sky-subtracted images are then flattened using observations of the continuum source in the interface box with the same instrumental configuration. Conventional spectral reduction software such as the IRAF 'apall' task are used to extract the spectrum. Because the 'apall' task bins the signal along the rows of the array, it was important to install the array with lines of constant wavelength aligned with the rows, as noted earlier. Because of the off-plane Littrow configuration, the dispersion and spectral axes are not perpendicular; the dispersion axis is tilted by 2.°75 with respect to the array column axis. This is of no consequence to the reduction, since the 'apall' task derives the extraction aperture by an empirical fit to the spectrum.

Wavelength calibration presents a special challenge. Because the fractional spectral coverage with Phoenix is only 0.5% observations of a conventional emission line source, such as the ThNeAr lamp, at a particular observational setup are unlikely to detect more than one or two lines. The OH airglow lines used for calibration of lower resolution spectroscopy are similarly sparse at the Phoenix resolution and are absent at wavelengths longer than 2.27 μm. As a result, neither of these techniques can reliably yield sufficient information for a reliable dispersion solution. The numerous telluric absorption lines throughout the near-IR compensate somewhat for their nuisance value by providing a reliable grid of calibration lines<sup>2</sup> at almost any wavelength setting of Phoenix. Removal of these telluric absorption features is an integral part of the data reduction process, so the observations of early-type stars necessary for this step of the reduction also provide the data for wavelength calibration.

Phoenix has been available to the KPNO user community since January 1997 and has been used for scientific programs over the entire 1 - 5 μm range for which the instrument was designed. The majority of the observations have been of point sources, for which the high spectral resolution is critical for measurements of radial velocity or abundances<sup>17</sup> or for identification of molecular species against a confusing background of strong telluric lines<sup>18</sup>. The usable slit length of 4.05 mm (150 pixels; 52 arcseconds at the 2.1 m) is sufficient for observations of moderately extended objects such as planets or circumstellar shells associated with obscured protostellar or post-AGB objects<sup>19</sup> as well as for solar and laboratory use<sup>20</sup>.

## ACKNOWLEDGMENTS

Funds for the development and construction of Phoenix were provided entirely by the NOAO instrumentation program. We thank NOAO director Dr. Sidney Wolff, associate director Dr. Richard Green, infrared group leader Dr. Ian Gatley, and head of engineering Mr. Larry Daggert for supporting the Phoenix project. We are indebted to those KPNO users who supported this project. We are especially grateful to Dr. Don Jennings who brought the R-C collimator design to our attention.

## REFERENCES

1. Hall, D. N. B., Ridgway, S. T., Bell, E. A. & Yarborough J. M. 1979, "A 1.4 Meter Fourier Transform Spectrometer for Astronomical Observations," SPIE 172 121
2. Hinkle, K., Wallace, L., & Livingston, W. 1995, "Infrared Atlas of the Arcturus Spectrum, 0.9-5.3  $\mu\text{m}$ ," San Francisco: Astronomical Society of the Pacific; Wallace, L. & Hinkle, K. 1997, "Medium Resolution Spectra of Normal Stars in the K-Band," ApJS 111 445
3. Ridgway, S. T. & Hinkle, K. H. 1993, "Strategies for Very High Resolution Infrared Spectroscopy," in High Resolution Spectroscopy with the VLT, ed. M.-H. Ulrich (ESO Conf. and Workshop Proceedings 40), p. 213
4. Bingham, R. G. 1979, "Grating Spectrometers and Spectrographs Re-examined," Quarterly Jour. R.A.S. 20 395
5. Optikos Software Corporation, 1993.
6. Harmer, C. personal communication
7. Hinkle, K. H., Drake, R. & Ellis, T. 1994, "Cryogenic Single-Crystal Silicon Optics," SPIE 2198 516
8. Schroeder, D. J. 1987, "Astronomical Optics," San Diego: Academic Press, p. 284-294.
9. Palmer, C. & Loewen, E. 1993, "Diffraction Grating Handbook," Rochester, New York: Milton Roy Instruments
10. Probst, R. G., Ellis, T. A., Fowler, A. M., Gatley, I., Heim, G. B., & Merrill, K. M. 1994, "Cryogenic Optical Bench: a Multifunction Camera for Infrared Astronomy," SPIE 2198 695
11. Ellis, T. et al. 1992, "The Simultaneous Quad-color Infrared Imaging Device," SPIE 1765 94
12. Vukobratovich, D. 1994 personal communication
13. Ellis, T., Little, J., & Christeler J. C., "Unique Design for Use of Closed-Cycle Refrigerators for Astronomical Observations," 1990, SPIE 1235 361
14. Fowler, A. M., Gatley, I., Vrba, F. J., Ables, H. D., Hoffman, A., & Woolaway, J. 1994, "Next Generation in InSb Arrays: ALADDIN, the 1024x1024 InSb Focal Plane Array Development Project Status Report," SPIE 2198 623
15. Heim, G. B., Buchholz, N. C., & Luce, R. W. 1994, "NOAO Wildfire Instrument Controller," SPIE 2198 1024
16. Joyce, R. R. 1992, "Observing with Infrared Arrays", in Astronomical CCD Observing and Reduction Techniques, ed. S. Howell, ASP Conference Series 23 258
17. Pilachowski, C., Sneden, C., Hinkle, K., & Joyce, R. 1997, "Carbon Isotope Ratios from the First Overtone CO Bands in Metal-Poor Giants," AJ 114 819
18. McCall, B. J., Geballe, T. R., Hinkle, K. H., & Oka, T. 1998, "Detection of  $\text{H}_3^+$  in the Diffuse Interstellar Medium towards VI Cyg 12," Science, in press
19. Weintraub, D. A., Huard, T., Kastner, J. H., & Gatley, I. 1998, "The Onset of Molecular Hydrogen Emission from Proto-planetary Nebulae," ApJ, submitted
20. Ram, R. S., Bernath, P. F., & Hinkle, K. H. 1998, "Infrared Emission of NH: Comparison of a Cryogenic Echelle Spectrograph with a Fourier Transform Spectrometer," J. Mol. Spec., in preparation